Volume 13, Number 2, 2020. pp. 113-121

Jordan Journal of Physics

ARTICLE

Impedance Spectroscopy and Dielectric Properties of Carbon Nanotube-Reinforced Epoxy Polymer Composites

Z. Samir[a], **S. Boukheir**[a,b], **R. Belhimria**[a], **M. E. Achour**[a], **N. Éber**[c], **L. C. Costa**[d] and **A. Oueriagli**[b]

[a] *Laboratory of Material Physics and Subatomic, Faculty of Sciences, Ibn Tofail University, BP 242, 14000 Kenitra, Morocco.*

[b] *Laboratoire LN2E, Faculté des Sciences, Université Cadi Ayyad, B.P. 2390, Marrakech, Morocco.*

[c] *Institute for Solid State Physics and Optics, Wigner Research Centre for Physics, Hungarian Academy of Sciences, H-1525 Budapest, P.O.Box 49, Hungary.*

[d] *Physics Department, University of Aveiro, 3810-193 Aveiro, Portugal.*

Doi : https://doi.org/10.47011/13.2.3

Received on: 08/08/2019; Accepted on: 29/12/2019

Abstract: The aim of this work is to investigate the electric properties of carbon nanotube-reinforced epoxy polymer composites, using impedance spectroscopy, in the frequency range from 1 Hz to 10 MHz and over the temperature range from 25 to 105 °C. The dielectric response was analyzed using the complex permittivity and the electrical modulus formalisms, depending on temperature and filler concentration in the polymer matrix. Furthermore, an equivalent circuit model is proposed to describe the impedance response of carbon nanotubes/epoxy composites. The impedance studies disclosed the appearance of grain and grain-boundary effects, as confirmed by the Nyquist plot.

Keywords: Carbon nanotubes, Composites, Impedance spectroscopy, Equivalent circuit model, Grain effect, Grain-boundary effect.

Introduction

The use of carbon nanotubes (CNTs) in polymer nanocomposites has received much attention due to their enormous potential to enhance or modify particular mechanical and electric properties [1, 2]. These possibilities include the use of CNTs as conductive filler in insulating polymer matrices and as reinforcement in structural materials [3-8]. The aspect ratio, the amount and the dispersion states of carbon nanotubes determine how easily CNTs can interact with each other to construct an interconnecting network of percolation able to transfer electrons and phonons to improve the properties of the nanocomposite [9-11]. On the other hand, epoxy resins are well established as advanced composites displaying a series of promising characteristics for a wide range of applications. So, CNT incorporation into epoxy resins results in carbon nanotubes / epoxy composites allowing many potential applications, ranging from microelectronics to aerospace [12-15].

As an extension of our recent research for exploring electrical properties [16-22], we report in this paper a detailed investigation of the dielectric and electrical properties of CNT-loaded epoxy polymers using impedance spectroscopy. Based on the obtained results, we

Corresponding Author: M. E. Achour **Email**: achour.me@univ-ibntofail.ac.ma

can readily make the following observations. On the one hand, the analysis of the behavior of complex electric modulus revealed the existence of two dielectric relaxation processes. One of these relaxations was associated with dipolar interactions at high frequencies, whereas the other, appearing at lower frequencies, was consistent with the interfacial polarization effect. On the other hand, an important thermoelectric phenomenon of transition was shown in this type of materials, below and above the conduction threshold (in our case the percolation threshold was found at x =2.7%), which is the positive temperature coefficient in resistivity effect (PTCR). In addition, we report the behavior of the impedance that reveals the presence of grain and grain-boundary effects confirmed by single and double arcs in the Nyquist representation.

Experimental

Materials

Multi-walled carbon nanotubes, with an outer diameter of about 50 nm, a length in the range of 10–20 μm and purity higher than 95 wt% (Cheap-Tubes, USA Laboratories), were selected in this work. The matrix used was an insulating epoxy matrix DGEBA (diglycidylic ether of bisphenol 1A) produced by A.W. Chesterton Company, Boston (USA). DGEBA had a DC electrical conductivity of the order of 1.4×10^{-14} Sm^{-1} and density of 1.19 g/cm^3. The CNTs were dispersed uniformly through the polymer matrix in different concentrations, before adding 1% of hardener to make each mixture cohesive. The CNT/DGEBA gelation took 5 minutes after pouring into the mold. Finally, the obtained samples were unmolded after a few hours.

Differential scanning calorimetry (DSC) was carried out using a DSC Q100 V9.9 Build 303 (TA Instruments Co-USA) programmed between 0 °C and 500 °C, at a heating rate of 5 °C /min. The results were used to determine the glass transition temperature of the composite for four selected nanotube concentrations besides the neat, undoped polymer. In our previous work [21], it was observed that the glass transition temperature decreased from 63 °C for the neat polymer to 58 °C for the sample with 5.0% CNT concentration. This decrease of the glass transition temperature can be attributed to the creation of a dense polymer package which is the result of this filler loading increase that affects the free volume of polymer.

Experimental Procedures

Electrical Impedance Spectroscopy Measurements

The impedance measurements on the samples were performed using a Novocontrol Alpha-A Analyzer combined with the ZG4 impedance interface, in a 4-wire arrangement in the frequency range of 1 Hz $< f <$ 10 MHz under isothermal conditions, at temperatures ranging between 25 °C and 105 °C. The solid samples in the form of discs with a diameter of 13 mm and thickness of 2 mm were placed between two parallel plated electrodes. The studied composite materials were modeled by a lumped circuit consisting of a resistor and a capacitor connected in parallel. Impedance analysis provides a simple method to determine various complex formulations: permittivity (ε^*), modulus (M^*) and impedance (Z^*). The complex impedance $Z^*(\omega) = Z'(\omega) + jZ''(\omega) = 1/(G(\omega) + jB(\omega))$ can be converted into the complex permittivity $\varepsilon^*(\omega) = \varepsilon'(\omega) - j\varepsilon''(\omega)$ by the relations:

$$\varepsilon'(\omega) = {B(\omega)d}/{\varepsilon_0 A\omega} \tag{1}$$

and $$\varepsilon''(\omega) = {G(\omega)d}/{\varepsilon_0 A\omega} \tag{2}$$

where $j = \sqrt{-1}$ is the imaginary unit, $\omega = 2\pi f$ is the circular frequency, A is the electrode area of the sample, d is its thickness and ε_0 is the permittivity of vacuum ($\varepsilon_0 = 8.85 \times 10^{-12}$ Fm^{-1}). The terms $G(\omega)$ and $B(\omega)$ are the conductance and the susceptance of the samples. The electrical modulus, $M^*(\omega)$, is defined in terms of the reciprocal of the complex relative permittivity, $\varepsilon^*(\omega)$:

$$M^*(\omega) = {1}/{\varepsilon^*(\omega)} = M'(\omega) + jM''(\omega) \tag{3}$$

where $M'(\omega)$ and $M''(\omega)$ are the real and imaginary parts of the electrical modulus which can be expressed by using the complex dielectric constants *via* the following relations:

$$M'(\omega) = {\varepsilon'(\omega)}/{(\varepsilon'^2(\omega) + \varepsilon''^2(\omega))} \tag{4}$$

$$M''(\omega) = {\varepsilon''(\omega)}/{(\varepsilon'^2(\omega) + \varepsilon''^2(\omega))} \tag{5}$$

Results and Discussion

Dielectric and Electrical Modulus Properties

The complex permittivity of the specific samples of x = 0.8% and x = 5.0% (x is the concentration of carbon nanotubes) is shown in Fig. 1 and Fig. 2, respectively, which depict the imaginary part and in the inset the real part of the complex permittivity as a function of frequency, for different temperatures. For the composite with a lower CNT volume fraction; i.e., x = 0.8% (Fig. 1), we can observe that a relaxation process is present, which is expressed by the maximum in the imaginary part of the complex permittivity and the inflection in the real part. The amplitude of this maximum increases as the temperature increases. The relaxation phenomenon is probably the result of the combination of two principal polarization mechanisms [23-25]. The first one corresponds to the dielectric properties of the polymer, which is generally attributed to the re-orientation of dipoles. The other mechanism is related to the CNT presence. This polarization mechanism causes an electric charge concentrated at the CNT/epoxy interface.

For the higher CNT volume concentration;, i.e., x = 5.0% (Fig. 2), the relaxation peak vanishes. Indeed, the material is characterized by the formation of an infinite cluster of CNT particles, which allows the displacement of electrons through large distances. Interfacial polarization phenomena on surfaces of the finite clusters can always exist, but they are masked by the process of conduction.

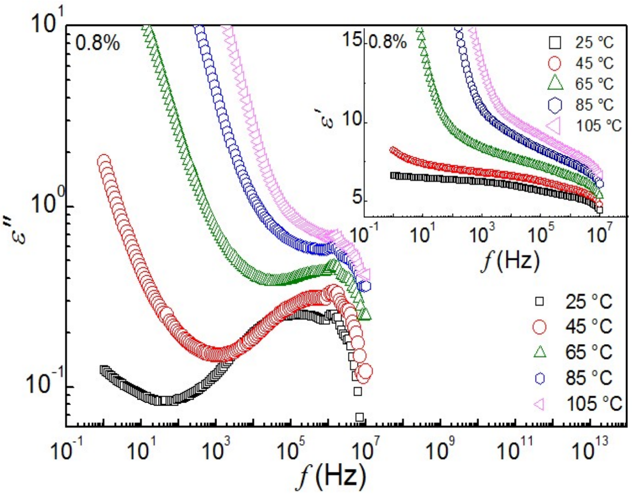

FIG. 1. Frequency dependence of the real and imaginary parts of the complex permittivity for various temperatures at the concentration of x = 0.8%.

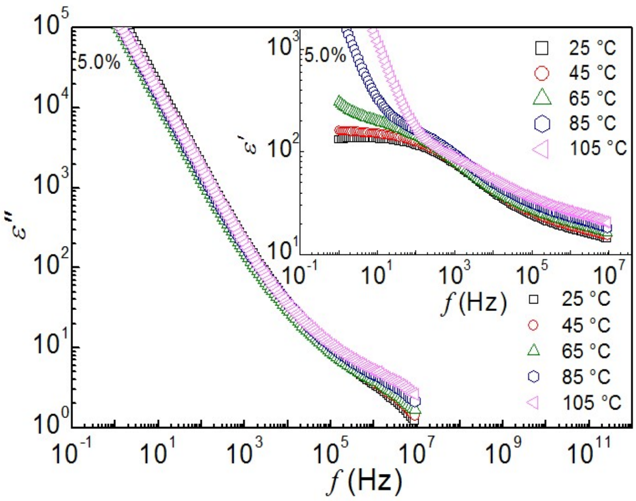

FIG. 2. Frequency dependence of the real and imaginary parts of the complex permittivity for various temperatures at the concentration of x=5.0%.

Figs. 3 and 4 show the modulus spectra for two CNT concentrations (x = 0.8% and x = 5.0%, respectively), at different temperatures. In Fig. 3, we observe the presence of one relaxation at the temperatures of 25 °C and 45 °C and the existence of two successive relaxations above the temperature 45 °C. The first relaxation, at high frequencies, represents the orientation of dipolar interaction groups, whereas the other, at low frequencies, is related to the interfacial polarization at the CNT/epoxy interfaces that gives rise to the Maxwell-Wagner-Sillars (MWS) polarization [26,27]. For x = 5.0% (Fig. 4), the two relaxations are superimposed giving a single distorted peak in $M''(\omega)$ at all temperatures.

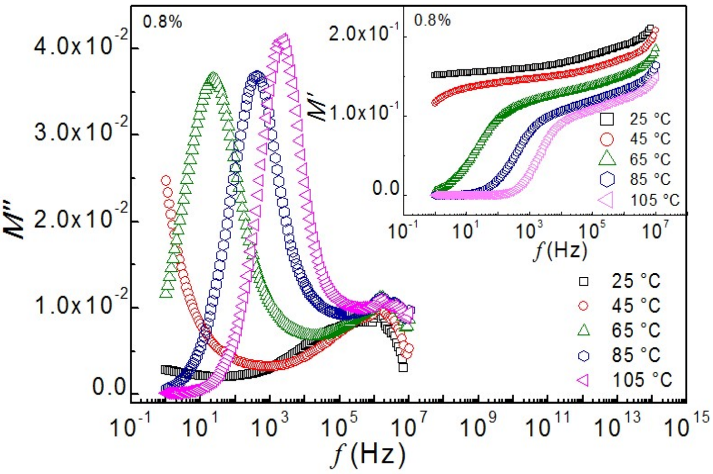

FIG. 3. Imaginary part of the electric modulus as a function of frequency for various temperatures at the concentration of x = 0.8%. The inset is a similar plot for the real part of the electric modulus.

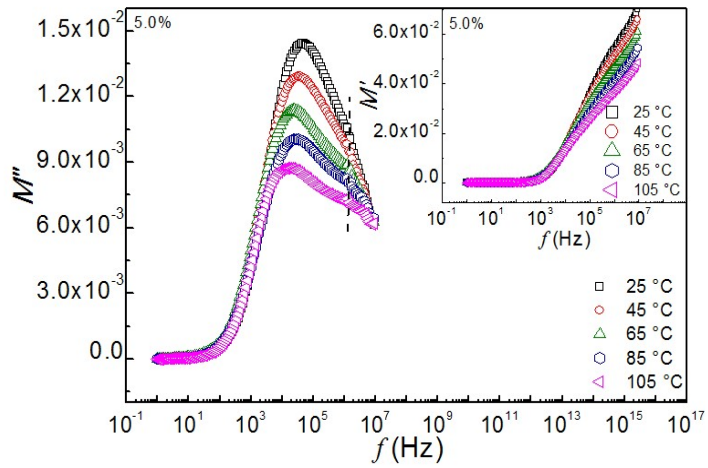

FIG. 4. Imaginary part of the electric modulus as a function of frequency for various temperatures at the concentration of x = 5.0%. The inset is a similar plot for the real part of the electric modulus.

Impedance Analysis

The impedance spectra of CNT/epoxy composites were analyzed by fitting to an equivalent electrical circuit which, instead of being a parallel R-C circuit, was the parallel combination of a resistance and a constant phase element (CPE) on the basis of brick-layer model [27–30]. The CPE was modeled as a non-ideal capacitor:

$$Z_{CPE} = {}^{1}\!/_{Q(j\omega)^n} \cdot \tag{6}$$

Here, Z_{CPE} is the impedance of the constant phase angle component, $0 < n < 1$ and Q is a constant. The CPE becomes equivalent to a capacitance when n = 1 [31]. This equivalent circuit model (Fig. 5a) is usable if only grain effect is present. If an additional grain-boundary effect is also to be taken into account, the equivalent circuit model has to be supplemented by a second, similar subcircuit of parallel R and CPE, connected in series (Fig. 5b). For the equivalent circuit models proposed, the total impedances Z_a and Z_b in the simple (Fig. 5a) and the extended (Fig. 5b) equivalent circuit models, respectively, can be expressed as:

$$Z_a = {R_g}/{(1 + R_g Q_g (j\omega)^{n_g})} \tag{7}$$

$$Z_b = {R_g}/{(1 + R_g Q_g (j\omega)^{n_g})} + {R_{gb}}/{(1 + R_{gb} Q_{gb} (j\omega)^{n_{gb}})} \tag{8}$$

Here, R_g and R_{gb} are the grain and the grain-boundary resistances, respectively, Q_g, Q_{gb}, n_g, and n_{gb} are constants.

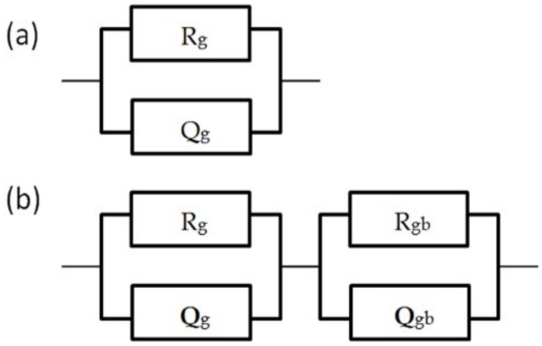

FIG. 5. Equivalent electrical circuits used to fit the impedance spectra of CNT/epoxy composites taking into account the effects related to (a) grain effect only, (b) both grain and grain-boundary effects.

To extract more information on the electrical responses and the structure-properties relationship, complex impedance spectroscopy is normally used. The Nyquist plots $Z''(Z')$ of the complex impedance for CNT/epoxy composites with 0.8% and 5.0% CNT content are shown in Figs. 6a-6b, respectively, for various temperatures from 25 °C to 105 °C. At room temperature measurements, no semicircle formation takes place. With increasing temperature, the behavior of Z'' *versus* Z' transforms into semicircles; this should be attributed to the grain effect in CNT particles (Fig. 6a) [32, 33]. In Fig. 6b, all the plots exhibit one single arc from room temperature (25 °C) to 85 °C representing grain effect only. When the temperature reaches 105 °C, a small segment of an arc appears at the low frequency side, which connects to the first semicircle. This suggests a process, in which the grain effect is gradually replaced by grain-boundary effect at increasing temperature [34]. It is also observed that the radius of the semicircles first increases, but then decreases with the increase in temperature, indicating a non-monotonic behavior of resistivity. Its depression at high temperatures is due to the statistical distribution of relaxation times.

Fig. 7 shows the temperature dependence of the maximum value Z''_{max} of the impedance $Z''_{max}(\omega)$ for the three concentrations. In Figs. 7b and 7c, it can be seen that Z''_{max} increased first with increasing temperature, which is obviously a positive temperature coefficient in resistivity (PTCR) effect, while negative temperature coefficient in resistivity (NTCR) effect appeared when the temperature was over 65 °C. For composites with 3.0% and 5.0% of CNT content, both the PTCR and the NTCR effects were very strong, while at 0.8% CNT content (Fig. 7a), only the NTCR effect was detectable. The PTCR could be attributed to volume expansion of the composites, which resulted in an increase of the distance between conductive tubes. However, the expansion could be paused when the distance of expansion was over the grid size of the cross-linked network in the rubber-matrix composites. With a further increase in temperature, electrons with enough energy could have an electron tunneling effect, which resulted in the NTCR effect.

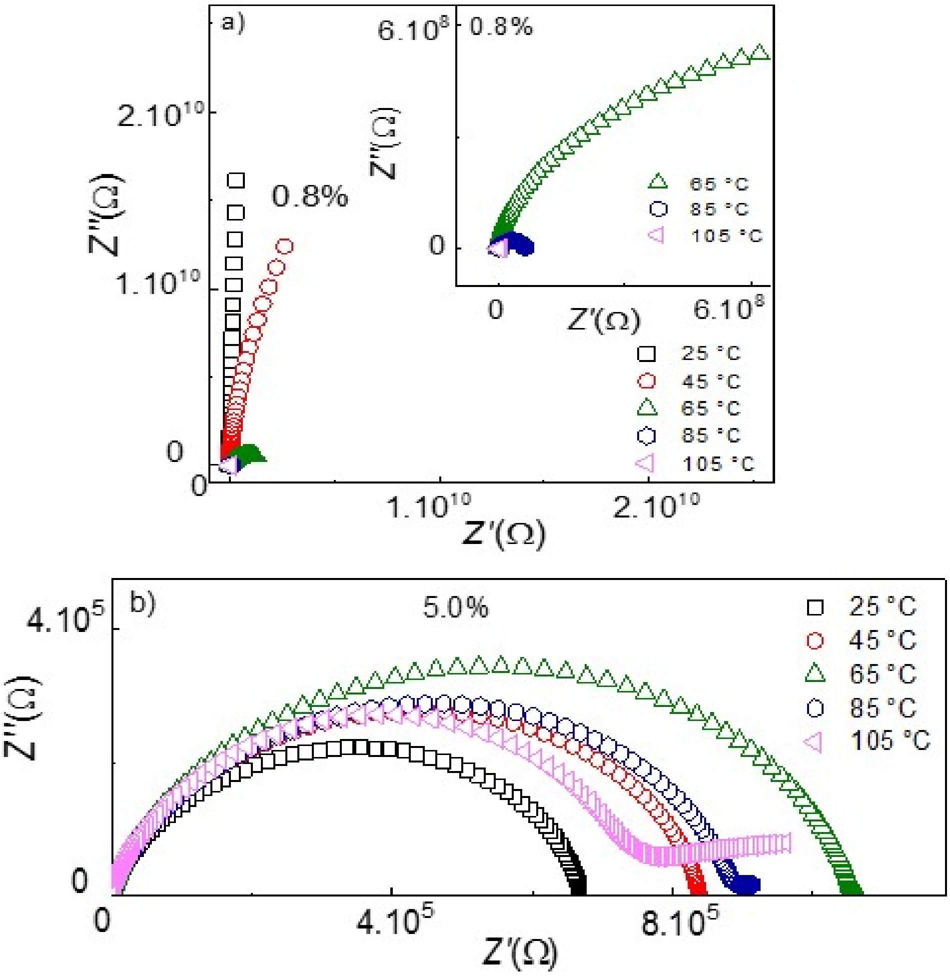

FIG. 6. Nyquist plots of the impedance of x = 0.8% (a) and x = 5.0% (b) CNT measured at different temperatures.

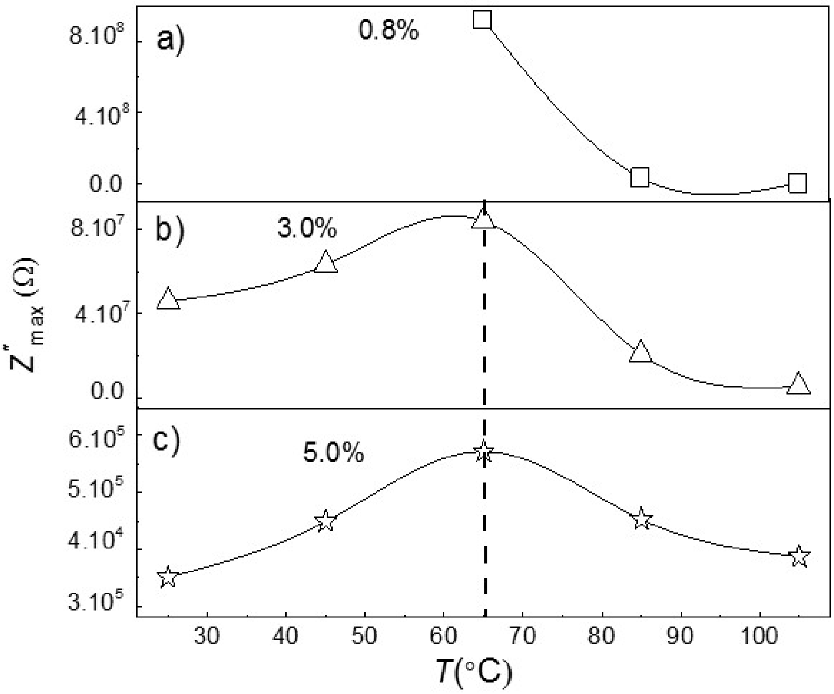

FIG. 7. Z''_{max} *vs*. temperature, for x = 0.8%, x = 3.0% and x = 5.0% CNT concentrations.

Fig. 8 compares the Nyquist plots of the complex impedance (symbols) with fitted data (solid line). For x = 0.8%, it is clearly shown that semicircular arcs are formed, whose shape remains almost the same as changing the temperature (Figs. 8a-8b). The experimental data was fitted with the impedance of the equivalent circuit in Fig. 5a, consisting of a parallel combination of a resistance and a CPE and representing the grain effect. For x = 5.0%, at low temperature (85 °C, Fig. 8c), the same equivalent circuit could be employed. However, at the higher temperature of 105 °C, a small segment of arc appeared from the low frequency side, which is connected to the first semicircle (Fig. 8d). This suggests a process, in which the grain effect is gradually replaced by the grain-boundary effect. In this case, the fitted curve was obtained using the extended equivalent circuit in Fig. 5b, consisting of two subcircuits in series that correspond to the two semicircular arcs. In addition, this also indicates that there exist two different relaxation processes and there is a distribution of the relaxation time rather than one particular relaxation time. The fitted parameters of grain and grain-boundary effects are tabulated in Table 1. The spectra reconstructed with the fitted parameters and the measured impedance spectra show good agreement with each other. Table 1 presents parameters also for CNT concentrations, whose spectra were not shown. From this table, it is found that the resistances R_g and R_{gb} decrease, while Q_g and Q_{gb} increase with CNT loading. The behavior for x = 2.5% was qualitatively the same as for x = 0.8%, while for x = 3.0%, it was similar to x = 5.0%.

TABLE 1. Fitted parameters of the Nyquist plots of CNT/epoxy composites with different CNT concentrations.

x (%)	T (°C)	R_g (Ω)	Q_g (F)	n_g	R_{gb} (Ω)	Q_{gb} (F)	n_{gb}
	25	-	-	-	-	-	-
0.8	65	1.72×10^{9}	7.45×10^{-11}	0.74	-	-	-
	105	7.47×10^{6}	7.89×10^{-11}	0.86	-	-	-
	25	-	-	-			
2.5	65	0.10×10^{9}	0.25×10^{-9}	0.74	-	-	-
	105	$1.72.10^{6}$	0.32×10^{-9}	0.80	-	-	-
	25	9.11×10^{7}	0.20×10^{-9}	0.79	-	-	-
3.0	65	0.15×10^{9}	0.21×10^{-9}	0.79	-	-	-
	105	1.05×10^{7}	0.16×10^{-9}	0.86	5.66×10^{6}	7.92×10^{-8}	0.56
	25	6.71×10^{5}	0.68×10^{-9}	0.76	-	-	-
5.0	65	1.60×10^{6}	0.89×10^{-9}	0.75	-	-	-
	105	7.35×10^{5}	0.57×10^{-9}	0.81	3.39×10^{5}	0.73×10^{-6}	0.54

Conclusion

The present work reports the results of our investigation on the electrical properties of CNT/epoxy composites. Both the permittivity and the modulus formalisms were used to interpret the relaxation processes at different temperatures. However, the electric modulus formalism was capable of revealing the interfacial relaxation which, in most cases, is covered by the conductivity of the material when represented in the dielectric. Positive temperature coefficient in resistivity and negative temperature coefficient in resistivity were also exploited, which is strongly dependent on the carbon nanotube content. A novel equivalent circuit model is proposed to describe the impedance response of the composites. The impedance measurements reveal the presence of grain and grain-boundary effects and confirm the temperature-dependent non-Debye type electrical relaxation processes in CNT/epoxy **composites.**

Acknowledgement

Financial support by the Moroccan (CNRST) - Hungarian (NKFIH) bilateral project TÉT_12_MA-1-2013-0010 as well as by the Budapest Neutron Centre (www.bnc.hu) is gratefully acknowledged. We also thank FEDER funds through the COMPETE 2020 Programme and National Funds through FCT - Portuguese Foundation for Science and Technology under the project UID/CTM/50025/2019.

References

[1] Breuer, O. and Sundararaj, U., Polym. Compos., 25 (2004) 645.

[2] Xie, X.L., Mai, Y.W. and Zhou, X.P., Mater. Sci. Eng. Rep., 49 (2005) 112.

[3] Allaoui, A., Bai, S., Cheng, H.M. and Bai, J.B., Compos. Sci. Technol., 62 (2002) 1998.

[4] Putz, K.W., Mitchell, C.A., Krishnamoorti, R. and Green, P.F., J. Polym. Sci. B., 42 (2004) 2293.

[5] Du, F., Fischer, J.E. and Winey, K.I., J. Polym. Sci. B., 41 (2003) 3338.

[6] Dai, J., Wang, Q., Li, W., Wei, Z. and Xu, G., Mater. Lett., 61 (2007) 29.

[7] Valentini, L., Puglia, D., Frulloni, E., Armentano, I., Kenny, J.M. and Santucci, S., Compos. Sci. Technol., 64 (2004) 33.

[8] Ounaies, Z., Park, C., Wise, K.E., Siochi, E.J. and Harrison, J.S., Compos. Sci. Technol., 63 (2003) 1646.

[9] Sandler, J., Shaffer, M.S.P., Prasse, T., Bauhofer, W., Schulte, K. and Windle, A.H., Polymer., 40 (1991) 5971.

[10] Ivanov, E., Kotsilkova, R. and Krusteva E., J. Nanopart. Res., 13 (2011) 3403.

[11] Jin, F.L. and Park, S.J., Carbon Lett., 14 (2013) 13.

[12] Pourzahedi, L., Zhai, P., Isaacs, J.A. and Eckelman, M.J., J. Clean Prod., 142 (2017) 1978.

[13] Verma, S., US Patents., 5,872,332A, Feb. 23, 1999.

[14] Albano, M., Micheli, D., Gradoni, G., Morales, R.B., Marchetti, M., Moglie, F. and Primiani, V.M., Acta Astronaut. 87 (2013) 39.

[15] Gooch, J.W. and Daher, J.K., "Electromagnetic Shielding and Corrosion Protection for Aerospace Vehicles", (New York, NY, USA: Springer, 2007).

[16] Samir, Z., El Merabet, Y., Graça, M.P.F., Teixeira, S.S., Achour, M.E. and Costa, L.C., Polym. Compos., 39 (2016) 1302.

[17] Samir, Z., El Merabet, Y., Graça, M.P.F., Teixeira, S.S., Achour, M.E. and Costa, L.C., J. Compos. Mater., 51 (2017) 1837.

[18] Boukheir, S., Len, A., Füzi, J., Kenderesi, V., Achour, M.E., Éber, N., Costa, L.C., Outzourhit, A. and Oueriagli, A., J. Appl. Polym. Sci., 134 (2016) 44514.

[19] Boukheir, S., Len, A., Füzi, J., Kenderesi, V., Achour, M.E., Éber, N., Costa, L.C., Outzourhit, A. and Oueriagli, A., Spectroscopy Letters, 50 (2016) 188.

[20] Samir, Z., Belhimria, R., Boukheir, S., Achour, M.E. and Costa, L.C., Jordan J. Phys., 11 (1) (2018) 35.

[21] Boukheir, S., Samir, Z., Belhimria, R., Kreit, L., Achour, M.E., Éber, N., Costa, L.C, Oueriagli, A. and Outzourhit, A., J. Macromol. Sci. B, 57 (2018) 221.

[22] Samir, Z., Boukheir, S., Belhimria, R., Achour, M.E. and Costa. L.C Journal of Superconductivity and Novel Magnetism, 32 (2019) 185. https://doi.org/10.1007/s10948-018-4696-6.

[23] Asami, K., Prog. Polym. Sci., 27 (2002) 165.

[24] Barucci, M., Bianchini, G., Gottardi, E., Peroni, I. and Ventura, G., Cryogenics, 39 (1999) 966.

[25] Achour, M.E., Salome, L., Benaboud, K., Carmona, F. and Miane, J.L., Adv. Mater. Res., 1 (1994) 468.

[26] Belattar, J., Graça, M.P.F., Costa, L.C., Achour, M.E. and Brosseau, C., J. Appl. Phys., 107 (2010) 124111.

[27] Mcclory, C., Seow, J.C. and McNally, T., Aust. J. Chem., 62 (2009) 785.

[28] Kolekar, Y.D., Sanchez, L.J. and Ramana, C.V., J. Appl. Phys., 115 (2014) 144106.

[29] Mohanty, S., Choudhary, RN.P., Padhee, R. and Parida, B.N., Ceram. Int., 40 (2014) 9025.

[30] Nayek, C., Murugavel, P., Kumar, S.D. and Subramanian, V., Appl. Phys. A, 120 (2015) 622.

[31] Orazem, M.E., Frateur, I., Tribollet, B., Vivier, V., Marcelin, S., Pébère, N. and Musiani, M., J. Electrochem. Soc., 160 (2013) C225.

[32] Sanli, A., Müller, C., Kanoun, O., Elibol, C. and Wagner, M.F.X., Compos. Sci. Technol., 122 (2016) 26.

[33] Messaoud, N.B., Ghica, M.E., Dridi, C., Ali, M.B. and Brett, C.M., Sens. Actuator B-Chem., 253 (2016) 522.

[34] Kumar, M., Shankar, S., Kumar, S., Thakur, O. P. and Ghosh, A.K., Phys. Lett. A., 381 (2017) 386.